Thermal Conductivity Measurement of Liquids in a Microfluidic Device

D. Kuvshinov[1], M. R. Bown[1], J. M. MacInnes[1§], R. W. K. Allen[1], R. Ge[2], L. Aldous[2], C. Hardacre[2], N. Doy[3], M. I. Newton[3] and G. McHale[3**]

[1]Chemical and Process Engineering, University of Sheffield
[2]School of Chemistry and Chemical Engineering, Queen's University Belfast
[3]School of Science and Technology, Nottingham Trent University, NG11 8NS, UK

Abstract

A new microfluidic-based approach to measuring liquid thermal conductivity is developed to address the requirement in many practical applications for measurements using small (microlitre) sample size and integration into a compact device. The approach also gives the possibility of high-throughput testing. A resistance heater and temperature sensor are incorporated into a glass microfluidic chip to allow transmission and detection of a planar thermal wave crossing a thin layer of the sample. The device is designed so that heat transfer is locally one-dimensional during a short initial time period. This allows the detected temperature transient to be separated into two distinct components: a short-time, purely one-dimensional part from which sample thermal conductivity can be determined and a remaining long-time part containing the effects of three-dimensionality and of the finite size of surrounding thermal reservoirs. Identification of the one-dimensional component yields a steady temperature difference from which sample thermal conductivity can be determined. Calibration is required to give correct representation of changing heater resistance, system layer thicknesses and solid material thermal conductivities with temperature. In this preliminary study, methanol/water mixtures are measured at atmospheric pressure over the temperature range 30 to 50 ºC. The results show that the device has produced a measurement accuracy of within 2.5% over the range of thermal conductivity and temperature of the tests. A relation between measurement uncertainty and the geometric and thermal properties of the system is derived and this is used to identify ways that error could be further reduced.

Keywords: liquid thermal conductivity measurement, resistance temperature sensor, microfluidic device, small sample volume.

[§] Corresponding author: Dr Jordan MacInnes; <u>j.m.macinnes@sheffield.ac.uk</u>; tel: +44(0)114 2227511
[**] NTU contact: <u>glen.mchale@ntu.ac.uk</u>; tel: +44(0)115 8483383

1. Introduction

Increasingly sophisticated application of microfluidic devices to chemical processing and analysis will require improvements in many areas, including on-chip measurement of liquid properties. Such measurements can provide crucial information for process operation and product quality control, as well as simply allowing rapid property determination in the case of uncharacterised liquids. Since properties can vary strongly with temperature, the ability to measure accurately over a broad temperature range is important. Here, we describe a novel approach to measuring liquid thermal conductivity in a microfluidic chip and report preliminary tests to determine its performance.

Measurement of liquid thermal conductivity with conventional techniques involving, typically, millilitre sample volumes may be unacceptable where the test liquid is available only in small amounts or is costly. Recent work (Gustavsson *et al.*, 2003, Kuntner *et al.*, 2006, Cheng *et al.*, 2006, Choi and Kim, 2008) has begun to examine the possibility of using microfabricated devices as the basis for liquid thermal conductivity determination and such devices should allow accurate measurements to be made using microlitre sample volumes. In each case, microfabrication methods are used to construct, what are in effect, miniature versions of established probe types.

Measurement techniques for thermal conductivity in solids, liquids and gases have developed steadily over the past sixty years following the early work reported in Carslaw and Jaeger (1959). Generally, a source of energy is introduced within the sample material and the resulting temperature response at one or more positions is recorded. The analytical solution of the heat conduction equation corresponding to the boundary conditions appropriate to the particular heating geometry is used to relate the measured temperature transient to the thermal conductivity of the sample material. Heating is variously introduced at a point (Hooper and Lepper, 1950), along a line (Van der Held and Van Drunen, 1949, Van der Held *et al.*, 1953, Nix *et al.*, 1967, De Groot *et al.*, 1974) or over a surface (Gustafsson *et al.*, 1979). Most commonly, heating is applied at a constant rate, but in other approaches heating is sinusoidal (Bruce and Cannell, 1976, Cahill, 1990, Choi and Kim, 2008). Further work has applied, refined and developed these approaches to improve accuracy and reliability (Filippov, 1966, Asher *et al.*, 1986, Gustafsson, 1991, Wang and Yang, 1995, Hammerschmidt, 2003, Hammerschmidt and Meier, 2006, Voudouris and Hayakawa, 1994, Zhang *et al.*, 2003 and 2005, Xie *et al.*, 2006). Particular issues addressed in the case of liquids include the effect of radiative heat transfer (Cahill, 1990, Gustavsson *et al.*, 2003) and the influence of natural convection associated with heating (De Groot *et al.*, 1974, Asher *et al.*, 1986, Gustavsson *et al.*, 2003).

In these approaches, the analytical solution used to determine the unknown thermal conductivity applies strictly for a sample region of infinite extent surrounding the heat source. Indeed, much of the early work (e.g. De Groot *et al.*, 1974) addresses the issue of how far radially (point or line source) or how far perpendicularly (surface source) the sample region must extend before it approximates with given accuracy an infinite region. Care in ensuring an adequately large sample region allows thermal conductivity to be measured with an accuracy approaching, and in some cases surpassing, 1%. Sample volumes depend on the heater dimensions and the mode of heating, but are typically in excess of 10 mL and sometimes much larger. For example in Gustavsson and Gustafsson (2006) a 4 mm diameter disk-shaped heating surface was used to measure the thermal conductivity of milk as a means of detecting changes in fat content. It was estimated that the 'active' sample volume was as little at 40 μL although the sample volumes actually used in the tests were 16 mL. But significant miniaturisation has begun with a 'hot strip' heater measuring 42 μm wide and 1.3 mm in length formed by sputtering gold onto a polymethylmethacrylate (PMMA) surface and used to make measurements in water and different

silicon oils (Gustavsson et al., 2003). In principle, the sample volume could be made as small as 2 µL, but again the actual tests are made by covering the active sensor area in a much larger volume of the sample liquid. Thus, while this approach shows considerable promise its integration with a suitable sample delivery system to allow measurements with minimal sample volume remains to be demonstrated.

Two recent studies use silicon fabrication methodologies to construct arrangements of heaters and temperature sensors for thermal conductivity measurement. In Kuntner *et al*. (2006) a 0.5 mm by 1.1 mm 'diaphragm' of approximately 1 µm thickness containing a line-source heater and temperature sensors is constructed from a 300 µm thick silicon wafer. Measurement is based on sinusoidal heating with the entire chip submerged in the sample liquid so that the heating and sensing elements are surrounded on both sides of the diaphragm by the sample liquid. The need for contact with the liquid on both sides of the diaphragm together with the fragility of the thin diaphragm is a possible limitation of the approach. The measurement accuracy for thermal conductivity is found to be in the range 8% to 26%. This large error may be the result of placing critical heat transfer regions too near to the highly conductive silicon that supports the diaphragm. A second study (Cheng *et al*., 2006) has used a similar fabrication approach to construct a diaphragm with an approximately point source of heating. Rather than operating with sample liquid on both sides of the diaphragm, a single 3 µL drop of liquid is placed over one side of the diaphragm to make a measurement. Issues of symmetrical and repeatable alignment of the drop with the heating and sensing elements, accounting for heat lost from the side of the diaphragm not in contact with the liquid and evaporation of volatile liquid specimens mean that the results obtained are uncertain. There is also concern about the suitability of the transformation from measured temperature transient to the thermal property (thermal diffusivity in this case). An exponential function is fitted to the recorded temperature and the time constant of the exponential is related to thermal diffusivity. However, the recorded time constant is found to increase with liquid diffusivity, which is opposite to expectation and this finding is presented without explanation.

These previous studies generally use an approach that assumes heat transfer in a three-dimensionally infinite medium. This requires both a large volume of sample liquid and places what may be impractical constraints on geometric details such as diaphragm thickness and size in the case of micro scale devices. An analytical framework is essential to enable a reliable transformation from measured quantities (usually a temperature transient) to a property such as thermal conductivity. However, the physical model being used in the measurement must satisfy adequately the conditions of the underlying analytical theory. One exception is the 3-ω method based on sinusoidal heating (Cahill, 1990) in which the sample volume required to give a satisfactory approximation of an infinite domain decreases as heating frequency increases. This method has been employed recently with promising results in Choi and Kim (2008) to measurement of thermal properties of liquid in a microchannel.

The approach presented here replaces the three-dimensionally infinite sample region with a thin planar layer of sample liquid. A large extent is then required only in the planar directions. With uniform heating from a parallel plane on one side of the layer, the thermal wave produced is detected by a resistance temperature sensor on the other side of the sample layer to allow determination of the thermal conductivity of the sample. Suitable design of the layer geometry ensures heat flow near the sensor is closely one-dimensional and three-dimensional and finite-reservoir effects can be easily removed. This is achieved by making the thermal time scale of the planar layers far smaller than those of the outer three-dimensional apparatus and thermal reservoirs. Because of this separation of time scales a purely one-dimensional transient can be isolated and the corresponding steady state temperature rise can be related to sample thermal

conductivity using simple theory. Thus, there are two steps in the present technique: first extracting the one-dimensional transient from the measured transient and second relating the steady temperature rise of the one-dimensional transient to sample thermal conductivity.

We investigate application of this approach to measurement of water/methanol mixtures (thermal conductivities from 0.2 to 0.6 W/m/K) over the temperature range 30 to 50 ℃, which corresponds to the range of temperature below the normal boiling point of methanol and for which our current oven can reliably control ambient temperature. Steady-state conduction theory is found to represent the relationship between temperature rise of the one-dimensional transient and thermal conductivity, but only when an account of changes to the system with temperature is included. Finally, the errors associated with the measurement are considered.

2. Theory

This section develops the relatively straightforward relationship between the steady state of the one-dimensional component of the transient and sample thermal conductivity. The measurement involves transient heat transfer through a stack of planar layers of material, one of which is the sample. The layers involved in the experimental apparatus are defined in Fig. 1. The glass chip sandwiches a layer of sample liquid and incorporates a thin metal layer on its top surface which can produce uniform heating by introducing electric current. The chip is in turn sandwiched between two copper reservoirs (not shown) with a polytetrafluoroethylene (PTFE) layer providing electrical and thermal insulation above the heater. It is assumed in the analysis that the initial temperature of the reservoirs, T_o, remains constant and uniform throughout the transient, i.e. that the reservoirs are infinite with infinite thermal conductivity. As mentioned, the finite-reservoir effects can be removed along with three-dimensional effects provided they are characterised by a much longer time scale than that of transmission through the chip and insulator layers shown in the figure.
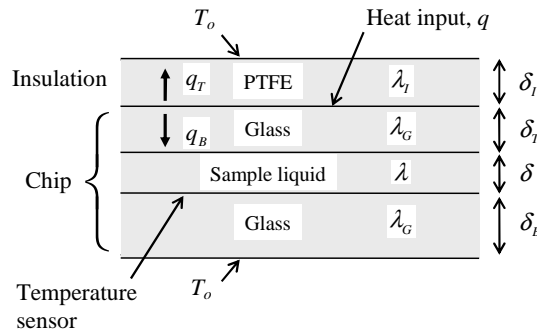

Figure 1. The one-dimensional arrangement of planar layers used to determine thermal conductivity of a sample liquid.

Starting with an initially uniform temperature, T_o, throughout the stack, a constant and known heating, q, is introduced. This heating is balanced by heat flux upward through the top of the stack, q_T, and downward through the bottom, q_B, (Fig. 1). For constant reservoir temperatures at the external boundaries equal to the initial temperature, T_o, a steady state of heat transfer is reached for which a relation can be derived between the temperature measured at any point in the stack and the unknown sample thermal conductivity. Here, the temperature is measured at the interface between the liquid sample and the bottom layer of glass forming the chip and the steady state relation is derived accordingly. The thermal resistance of the PTFE layer and the combined resistance of the glass and sample layers determine the relation between heat fluxes in the two directions at steady state:

$$\frac{\delta_I}{\lambda_I} q_T = \left(\frac{\delta_T + \delta_B}{\lambda_G} + \frac{\delta}{\lambda} \right) q_B \qquad (1)$$

Defining the temperature at the measurement location relative to the initial ambient, $\Delta T = T - T_o$, the heat flux through the bottom of the stack at steady state is:

$$q_B = \frac{\lambda_G \Delta T}{\delta_B} \qquad (2)$$

Using $q = q_T + q_B$ to eliminate q_T, and Eq. 2 to eliminate q_B, in Eq. 1 gives the final relation between stack properties, heat input and the steady state temperature difference at the sensor:

$$\lambda = \frac{1}{\dfrac{\alpha}{\Delta T} - \beta} \qquad (3)$$

The coefficients α and β are functions of the layer thicknesses, the thermal conductivities of the solid layers and the heating rate given by

$$\alpha = \frac{q \delta_B \delta_I}{\delta \lambda_G \lambda_I} \qquad (4)$$

$$\beta = \frac{1}{\delta} \left(\frac{\delta_I}{\lambda_I} + \frac{\delta_T + \delta_B}{\lambda_G} \right) \qquad (5)$$

For fixed layer thicknesses, fixed thermal conductivities in the solid layers and fixed heating rate, α and β are constant and independent of the sample properties. Thus, from Eq. 3, measurement of the steady state temperature difference, ΔT, determines the unknown sample conductivity.

3. Experiment

The liquid sample layer in Fig. 1 is approximated in the actual apparatus by a cylindrical volume of radius 3.75 mm and depth 125 μm and this is incorporated in a 3x3 cm by 1 mm thick glass chip fabricated by Micronit Microfluidics. The chip is formed from two layers of glass, the upper layer 300 μm thick and the lower 700 μm thick. Flow passages and the sample cell are formed by wet etching (to 125 μm depth) into the under side of the upper layer with connection holes powder blasted through this layer. The heater is formed by deposition of a 10 nm tantalum layer followed by 180 nm of platinum on the top surface of the upper layer. The temperature sensor circuit is similarly formed on the upper surface of the lower glass layer, before the two layers are thermally bonded to produce the final chip. The resistance sensor comprises three wires of width 10 μm and 1.4 mm length in series (Fig. 2c).

To complete the apparatus, the chip is clamped in a holder between a lower 5 mm thick plate of copper and an upper 15 mm block of copper, with a 208 μm thick insulating PTFE layer placed between the copper block and the upper chip surface. The holder incorporates flow fittings for capillary connections and spring pins for electrical connections. Fig. 2 shows a schematic diagram of the chip and holder arrangement, a photograph of the assembly and detail of the sensor. The sample liquid is introduced using a neMESYS syringe pump (Cetoni GmbH) and syringe connected through a 0.2 μm filter and 150 μm ID capillary tubing. During the experiment

the chip holder assembly is placed in a custom built convection oven which allows accurate control of the ambient temperature in the range from about 30 ºC up to the material limits of the chip holder. In addition to the temperature sensor in the chip, two small thermocouples are used to monitor temperature at central locations in the copper reservoirs.
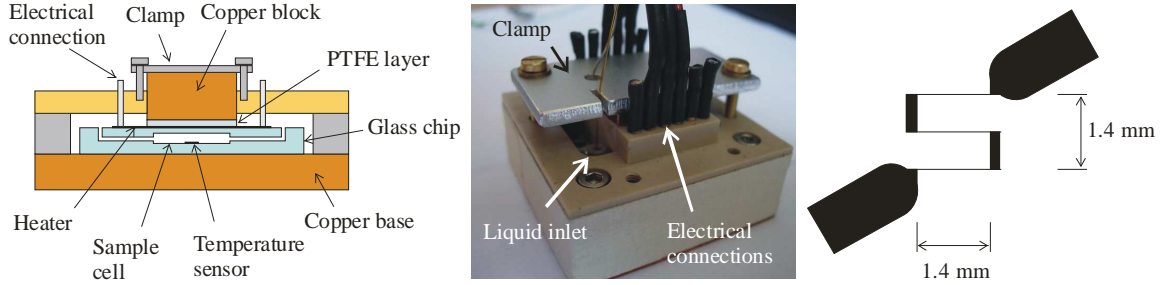

Figure 2. (a) Schematic section diagram of the glass chip and holder. (b) The actual chip and holder assembly showing the clamp, the inlet flow connection and electrical connections for heating and temperature sensing. (c) Geometry of the resistance element used to sense temperature.

The layer thicknesses used in the chip are based on the results of a parametric study using numerical solution of the time-dependent heat conduction equation for both the one-dimensional case and also a two-dimensional approximation of the combined holder and chip apparatus. The heat equation ($\rho C_P\, \partial T/\partial t = \lambda \nabla^2 T$) is solved throughout the solid and liquid regions subject to either external constant temperature or heat transfer coefficient boundary conditions and with flux and temperature continuity imposed at the interfaces between different solid and liquid regions. (The computations make use of the commercial software packages Fluent 6 and Comsol 3.)

The plot of Fig. 3 shows example results for the temperature response at the sensor position in both one-dimensional and two-dimensional computations using a heat transfer coefficient to represent external boundary conditions. The continual rise in temperature beyond the initial 1 s of time is indicative of gradual filling of the copper layer reservoirs impeded by the resistance associated with the external heat transfer coefficient. The slower rise for the two-dimensional geometry is the expected result of the larger reservoir volume per heated surface in that case. The important feature to note is that the initial temperature transients for the one and two dimensional cases are identical. Were a constant temperature held at the external boundaries of the copper layers there would be no continuing rise in the temperature and a steady state value would be reached after just a few seconds. It is this temperature rise which allows the thermal conductivity to be determined. The temperature rise is reduced by the multidimensional effects as heat can bypass the sample layer by flowing around the sample volume through the surrounding glass. One- and two-dimensional computations were made using constant temperature boundary conditions to quantify the reduction in temperature and to establish the conditions required to give a good approximation to one dimensional heat transfer along the axis, i.e. at the position of the temperature sensor position in the apparatus. The reduction in the temperature rise will clearly decrease as the sample cell radius is increased, but it was also found that the thickness of the top glass layer strongly influences the one-dimensionality of the heat flow. A thinner top glass layer, relative to the sample layer thickness, brings the heat transfer affecting the sensor temperature nearer to one-dimensionality. For the chip dimensions selected for the apparatus it is estimated from the computational study that the temperature detected at the sensor position at steady state will be just 2% lower than for precisely one-dimensional heat transfer.
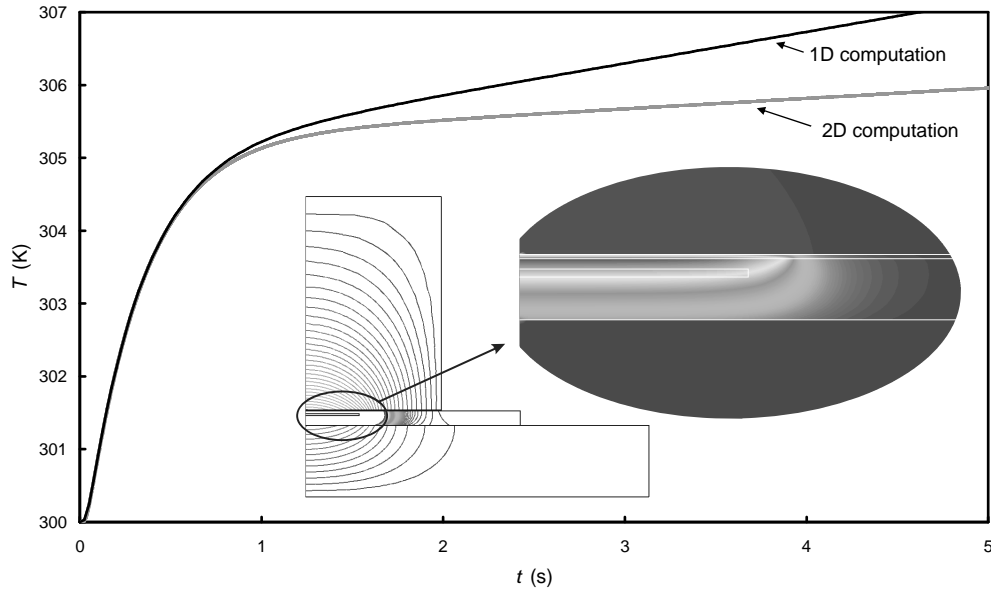
6

Figure 3. Example computation of temperature transient at the sensor position showing the effect at long time of two-dimensionality. Insets show computed isotherms near steady state in a two-dimensional axisymmetric geometry. The axis of symmetry is on the left hand sides in these insets and the glass chip and the top and bottom copper reservoirs can be seen. In the shaded inset, the region occupied by the liquid sample can be seen and the one-dimensionality of the temperature field in the central region near the symmetry axis (sensor position) is evident.

From information given above, the layer thicknesses appearing in the steady state theory take the values $\delta = 125$ μm, $\delta_T = 175$ μm, $\delta_I = 208$ μm, $\delta_B = 700$ μm. While the final two dimensions are accurate to small fractions of a percent, the first two are determined by the wet etching and are believed to be uncertain by around 2%. All but the etching depth were measured using a digital micrometer (1 μm precision). Etched depth was measured more approximately using microscopy (MacInnes *et al.*, 2003).

A second practical issue involves conditions of the insulation layer needed to ensure the time scale of the one-dimensional transient remains small. The relatively small conductivity of the PTFE insulation requires that layer in particular to be thin so that the one-dimensional transient can be easily separated from the more complex transient effects associated with the finite size of the copper reservoirs, the three-dimensionality of the outer apparatus and the external boundary conditions. The heater has been made by metal deposition and has uniform resistivity per unit area. The heating area is a strip 9 mm wide, i.e. just wider than the cell diameter, and extending the length of the chip. Electric current is passed to the strip through two spring pin connectors at either end. Numerical solution of the two-dimensional Laplace equation for electric potential has been used to determine that the electric field, and hence heating rate per unit area, is uniform to within 1% in the region of the heater directly over the sample cell.

Temperature is measured using resistance change of a serpentine element (Fig. 2c) giving electrical resistance of $R = 540$ Ω at 20 °C and fitting into a 1.4 mm square region at the bottom centre of the sample cell. The change in sensor resistance with temperature is detected by measuring voltage across a reference resistor (1 kΩ) in series with the sensor when constant voltage is applied across the two resistances. Over the temperature range of the measurements, the expected linear relation between temperature and resistance has been found to apply, i.e. $R = aT + b$. This relation is used to transform from measured sensor resistance to temperature. Estimates show that the additional heating associated with sensor operation introduces only about

3% of the heating per unit area of the heater itself and should have a negligible effect on the thermal transient. Moreover, the sensing is begun well in advance of the start of heating and so the temperature field associated with the sensor heating is approximately at steady state and the temperature transient at the sensor relative to the initial temperature there is expected to be independent of the pre-existing steady temperature field.

Radiative heat transfer is neglected from the theory resulting in Eqs. 3, 4 and 5. Estimates of its magnitude at the conditions used in the tests indicate that this approximation is indeed justified, with radiative flux being less than 0.5% of the conductive flux of heat within the chip layers.

The measurement is controlled by computer using a LabVIEW 8.6 program which, following adjustment of the oven to the required ambient temperature, records temperature for 1 s to establish the initial ambient condition, switches the heater on to start the transient (constant voltage applied to the heater resistance), shuts off the heater and sensor after 12 seconds of data recording and saves the data to complete the measurement. Sensor voltage is recorded every 3 ms which corresponds to the highest acquisition rate for the hardware used.

4. Results

A typical sequence of sensor temperatures measured during the heating transient is shown in Fig. 4. The data are plotted after subtracting the value of the initial ambient temperature, T_o, determined by averaging temperature over a 1 s period ending 100 ms before the heater is switch on. There is an initial rapid rise in the temperature followed by a continuing constant rate of increase. This is similar to that found in the computations (Fig. 3) and suggests successful separation of the time scale for the one-dimensional transient and that of overall apparatus. The part of the transient associated with one-dimensional heat transfer would be expected to have an analytical representation corresponding to an infinite series of exponential terms, each successive term having a smaller time constant than the previous (e.g. Berg and McGregor, 1966). Typically, after a short time all but the fundamental exponential term become negligible. In our case, we expect terms with very short time scale defining the delay in arrival of the thermal wave, a single one-dimensional fundamental mode of intermediate time scale (the fundamental of the one-dimensional component) and remaining modes of much greater time scale. Therefore, it is not surprising to find that the experimental data are closely fitted by the sum of a single exponential rise corresponding to the one-dimensional fundamental mode and a linear term representing the linearised exponential terms of the slow filling of the reservoirs and three-dimensional effects:

$$T(t) - T_0 = \Delta T\left(1 - \exp\left\{-\frac{t - t_0}{\tau}\right\}\right) + \gamma(t - t_0) \qquad (6)$$

This function is fitted to the data using a least squares technique and the result for the particular data shown in Fig. 4 is plotted as a white line over the data on the figure. The fit involves adjustment of the three parameters: steady state temperature rise at the sensor position, ΔT, time scale of the one-dimensional fundamental, τ, and slope of the long-time modes, γ. It can be seen from the figure that Eq. 6 captures the mean of the data strikingly well and this was found for all conditions tested.[††]

[††] Eq. 6 uses a time shift, t_o, in place of actual short-time exponential terms to represent the delay in the arrival of the thermal wave to the sensor position. It is interesting to note that the alternative fitting function using just a single additional short time exponential mode:
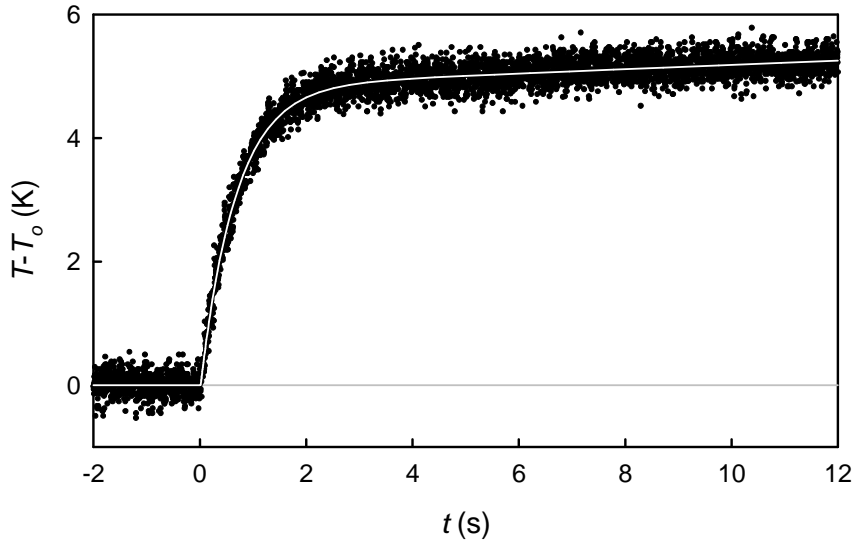
Figure 4. Data (symbols) collected from the temperature sensor during the initial transient following the start of heating. The white line passing through the data is Eq. 6 giving a least squares fit of the data.

Preliminary assessment of the measurement approach used mixtures of water and methanol at three different temperatures, 30, 40 and 50 ℃. The mixtures tested were 0%, 25%, 50% and 100% methanol (by mass) in water giving a wide range of conductivity, from about 0.2 to 0.6 W/m/K. The temperature range was limited by the atmospheric boiling point of pure methanol and by the oven which controls the ambient temperature reliably for T_o greater than about 30 ℃. Data have been recorded at each of the twelve conditions in groups of six with each transient in the group separated by six minutes to allow the temperature field within the chip and holder to relax from the previous heating transient. Three groups of data were taken at each combination of temperature and mixture composition giving at least 16 separate measurements at each of the twelve conditions. All conditions include independent measurements, i.e. taken on different days with changed sample material and with the apparatus fully shut down in between measurements.

From each measured transient the value of ΔT is determined by a least squares fit of Eq. 6 and then λ is obtained using the one-dimensional theory, Eqs. 3-5. In that theory the layer thicknesses are those measured at approximately 20 °C and the thermal conductivities of the solid layers are taken from the CRC Handbook of Chemistry and Physics (2005) at the mid-range temperature of 40 °C. There is uncertainty regarding the true value of the heating rate, q, because the effective contact diameter between the spring pins and the platinum heater layer is not known. Thus, the heating rate was adjusted to give best overall fit with the known values of thermal conductivity in each mixture at each temperature from the literature (Assael et al., 1989, CRC Handbook, 2005). These data result from transient hot wire (line source of heating) measurements with an estimated accuracy of 0.5%. The value of the heating rate determined in this way (1.63×10^4 W/m^2) corresponds to an effective pin contact diameter of 0.53 mm, which is plausible for contact between the 1.8 mm diameter rounded pin tip pressed against the flat metal layer of the heater.

$$T(t) - T_0 = \Delta T_1 \left(1 - e^{-t/\tau_1} \right) - \Delta T_2 \left(1 - e^{-t/\tau_2} \right) + \gamma t$$

gives an equally good fit to the data. This could be used in place of Eq. 6 with the steady state temperature rise given by $\Delta T = \Delta T_1 - \Delta T_2$.

Fig. 5 shows a plot of the measured values of λ, derived from ΔT in this way, plotted against the actual values of thermal conductivity. The average of the measurements at each condition is plotted using different symbols for the different values of initial temperature. The error bars indicate the standard deviation of the measurements at each condition of mixture composition and initial temperature. Ideal measurement corresponds to the dashed line of unit slope shown in the figure and the measured values of λ stray considerably from this line and show a systematic deviation with initial temperature. The measurement overestimates the sample thermal conductivity at low initial temperature and underestimates it at high initial temperature. Noting that the actual thermal conductivity of a given mixture changes little over the range of initial temperature spanned by the experiments, the large variation in measured thermal conductivity with initial temperature shows that ΔT will change even when the sample properties remain fixed. Such changes in ΔT must, therefore, result from changes in layer thicknesses, the solid thermal conductivities and the heating rate with temperature. Of course, the thermal and electrical conductivities and the dimensions of a solid do change slightly with temperature and evidently these changes have a strong effect and must be taken into account. Eq. 3 gives increasing thermal conductivity with ΔT and so the system is changing with initial temperature in such a way that the recorded ΔT decreases with increasing initial temperature, Fig. 5. Precisely how the system is changing to cause this will be a complex interaction between thermal expansion in the parts of the system, changes with temperature of the conductivities of the solids and change in heater resistance. For purposes of measuring the thermal conductivity of a sample liquid, the crucial thing is that the system variations with temperature are repeatable, are insensitive to the sample properties (which alter slightly the temperature distribution in the solid regions) and can be included in the relation between thermal conductivity and ΔT.
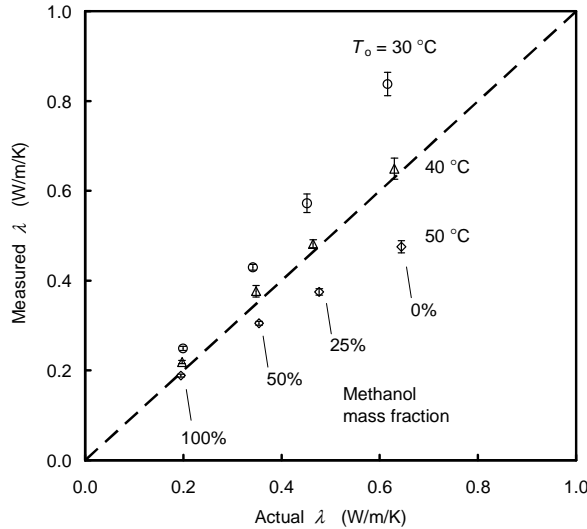

Figure 5. Comparison of measured and actual thermal conductivity. Measured ΔT is transformed to thermal conductivity using Eqs. 3, 4 and 5 with layer thicknesses measured at room temperature, thermal conductivities of solid layers from the literature [28] and a constant heating rate. Actual thermal conductivity values at the various temperatures and compositions are taken from [28,29]. All 202 measurements (at the four different methanol-water compositions and three initial temperatures, T_o) are included in the plot.

Noting that the system changes manifest themselves just by changes in the values of parameters α and β in the theory (Eqs. 4 and 5) it is possible that replacing these parameters by simple functions of temperature may suffice. After testing linear, quadratic and cubic polynomials it was found that the quadratic allowed a close fit to the data, with the linear polynomial proving inadequate and the cubic not noticeably improving the fit. Thus, the true dependence of α and β on the detailed changes in conductivities and layer thicknesses with temperature is replaced here by quadratic functions of T_o:

$$\alpha = AT_o{}^2 + BT_o + C \qquad\qquad (7)$$

$$\beta = DT_o{}^2 + ET_o + F \qquad\qquad (8)$$

The constants A, B, C, D, E and F are determined by least squares fit using all the data at all the temperatures and compositions. The resulting fit is plotted in Fig. 6 for the three particular values tested in the experiments. The rms deviation between the values of thermal conductivity given by the fitting function evaluated at the average ΔT of the data at each condition and the literature values is 1.3%, with maximum and minimum deviations found to be 2.5% and 0.2%, respectively. This gives an indication of the inaccuracy of Eqs. 3, 7 and 8 for this particular device. Clearly, the use of the quadratic variation in the coefficients in the one-dimensional theory captures well the temperature sensitivity of the system and the response of the system to sample thermal conductivity. This is confirmed by re-plotting the results in the same way as for Fig. 5, but including the temperature dependence. The result is shown in Fig. 7 and clearly the data now collapse to near the ideal line of perfect accuracy. Interestingly, the scatter in the measurement, which can be seen easily in this figure, increases with increasing λ and the cause of this is identified in the next section.
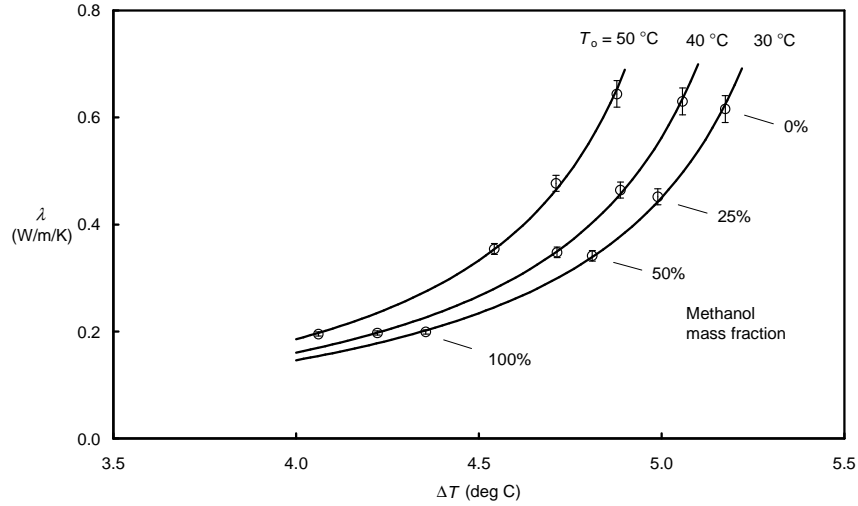

Figure 6. Actual values of thermal conductivity plotted at the mean ΔT for each temperature-composition condition compared to the theory with calibrated quadratic dependence of coefficients.
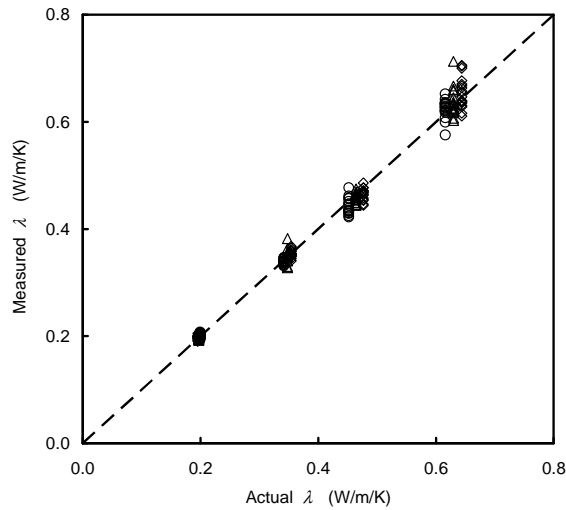

Figure 7. Comparison of measured and actual thermal conductivity with measured ΔT transformed to thermal conductivity using Eq. 3 with the quadratic dependence on temperature (Eqs. 7 and 8).

11

The α and β functions (Eqs. 7 and 8) fitting the data well give an approximately constant level of β but significant decrease in α with increasing T_o. Much of this change in α can be attributed to changing heating rate with temperature associated with increasing electrical resistance of the heater (voltage applied to the heater remains constant). Increased resistance then causes reduced heating power and hence α is expected to decrease with temperature (Eq. 4). However, this effect alone does not capture all of the change with temperature and effects of changing thermal conductivities of the solid materials and layer thicknesses are embodied in the α and β functions of temperature.

Finally, it must be noted that the measurements here have been made over a relatively narrow range of temperature and it remains to be seen whether the approach used here continues to apply over broader temperature ranges which will be of interest. We have in continuing work successfully extended the range down to 0.1 W/m/K which represents the lower end of the range of values expected for liquids. Also, it is possible to adjust the design to optimise the measurement for either higher or lower thermal conductivity ranges.

5. Measurement uncertainty

The uncertainty in λ for an individual measurement can be determined based on estimated uncertainties of the two measured quantities on which λ depends, i.e. ΔT and T_o. The standard deviations estimated from repeated measurements a given condition are $e_{\Delta T}$ =0.017 K for ΔT and e_{To} = 0.08 K for T_o. These random errors combine (e.g. Doebelin, 1975) using Eqs. 3, 7 and 8 to produce the following relation for the resulting standard deviation, e_λ, in λ.

$$e_\lambda = \lambda^2 \sqrt{\left(\frac{\alpha}{\Delta T^2} e_{\Delta T}\right)^2 + \left(\left[\frac{2AT_o + B}{\Delta T} - 2DT_o - E\right] e_{T_o}\right)^2} \qquad (9)$$

The second term in the square root is the contribution due to the T_o measurement uncertainty and is negligible because of the relatively minor sensitivity of λ to temperature. The first term in the square root is approximately constant for the same reason (since β is nearly constant). Thus, Eq. 9 shows that the relative uncertainty in measured thermal conductivity, e_λ/λ, is roughly proportional to the thermal conductivity. For the experiments, the full equation gives a relative uncertainty rising from 1.8 to 3.8% as λ changes from 0.2 to 0.6 W/m/K.

It is worthwhile considering the potential for reducing the measurement uncertainty. Since λ depends weakly on T_o, the second term in Eq. 9 can be dropped and ΔT expressed in terms of λ (using Eq. 3) to give:

$$\frac{e_\lambda}{\lambda} = \frac{\lambda}{\alpha}\left(\beta + \frac{1}{\lambda}\right)^2 e_{\Delta T} \qquad (10)$$

For the prototype design, β is approximately 15 m K/W (Eq. 5) which is large relative to sample values of $1/\lambda$. Thus, the error can be reduced by reducing β, for example by making the layer thicknesses smaller in relation to that of the sample layer or thermal conductivities of solid layers larger. Practically, β can probably be reduced by around 60% for chips fabricated from glass and this corresponds to a reduction in the relative uncertainty to 0.5% for λ =0.2 W/m/K and 0.7% for 0.6 W/m/K. (Note that this reduction corresponds to unchanging α as β is decreased which requires the heat input to increase as the parameters which allow β to decrease are altered.) Further reductions in the error would result from using silicon fabrication methods where layer

thicknesses could potentially be reduced even further. Such reductions in layer thickness also reduce required sample volumes. A second way to reduce the uncertainty is to reduce $e_{\Delta T}$. This should be possible with improved control of the noise affecting the sensor output.

6. Conclusions

A new microfluidic-based approach for measuring liquid thermal conductivity is developed and successfully tested. The compact micro device uses integrated heating and temperature sensing to produce and detect a thermal wave passing across a microlitre liquid sample. The device design facilitates the separation of a one-dimensional mode from the overall temperature transient and this allows sample thermal conductivity to be determined using simple conduction theory.

The results obtained show that the device response varies with temperature and this is due to temperature dependence of heater resistance, layer thicknesses and thermal conductivities of the solid materials comprising the device. It is found that a quadratic dependence of the overall coefficients in the conduction theory captures satisfactorily the device dependence on temperature.

The results for methanol-water mixtures at temperatures in the range 30 to 50 ℃ indicate that liquid thermal conductivity measurement has been achieved with an accuracy of 1.3% and an uncertainty of between 1.8 and 3.8%, depending on the value to be measured. Analysis of the error shows that it is possible to reduce the error further by reducing layer thicknesses and/or reducing temperature measurement uncertainty.

The approach developed addresses a range of possible applications in the biomedical, pharmaceutical and hazardous materials processing areas where high-throughput, fast-response testing and microlitre sample size are important.

References
1. Asher, G. B., E. D. Sloan and M. S. Graboski, 1986, "A Computer-Controlled Transient Needle-Probe Thermal Conductivity Instrument for Liquids", International Journal of Thermophysics, 7 (2), 285-294.
2. Assael, M. J., E. Charitidou and W. A. Wakeham, 1989, "Absolute Measurements of the Thermal Conductivity of Mixtures of Alcohols with Water", International Journal of Thermophysics, 10 (4), 793-803.
3. Berg, P. W. and J. L. McGregor, 1966, "Elementary Partial Differential Equations", Holden-Day, San Francisco.
4. Bruce, R. H. and D. S. Cannell, 1976, "Accurate Method for the Simultaneous Determination of the Thermal Conductivity and Specific Heat of Nonconducting Solids", Review of Scientific Instruments, 47 (12), 1323-1330.
5. Cahill, D. G., 1990, "Thermal Conductivity Measurement from 30 to 750 K: the 3ω Method", Review of Scientific Instruments, 61 (2), 802-808.
6. Carslaw, H. S. and J. C. Jaeger, 1959, "Conduction of Heat in Solids", 2nd Edition, Oxford University Press.
7. Cheng, Y.-T., C.-W. Chang, Y.-R. Chung, J.-H. Chien, J.-S. Kuo, W.-T. Chen and P.-Hei Chen, 2006, "A Novel CMOS Sensor for Measuring Thermal Diffusivity of Liquids", Sensors and Actuators A, 135, 451-457.
8. Choi, S. R. and D. Kim, 2008, "Real-time characterization of 12 nl fluid samples in a microchannel", Review of Scientific Instruments, 79, 064901, 1-5.
9. CRC Handbook of Chemistry and Physics, 86th ed., 2005, Taylor and Francis.
10. De Groot, J. J., J. Kestin and H. Sookiazian, 1974, "Instrument to Measure the Thermal Conductivity of Gases", Physica, 75, 454-482.
11. Doebelin, E. O., 1975, "Measurement Systems, Application and Design", Revised Edition, McGraw-Hill.
12. Filippov, L. P., 1966, "Methods of Simultaneous Measurement of Heat Conductivity, Heat Capacity and Thermal Diffusivity of Solid and Liquid Metals at High Temperatures", International Journal of Heat and Mass Transfer, 9, 681-691.

13. Gustafsson, S. E., E. Karawacki and M. N. Khan, 1979, "Transient Hot-Strip Method for Simultaneously Measuring Thermal Conductivity and Thermal Diffusivity of Solids and Fluids", Journal of Physics D: Applied Physics, 12, 1412-1421.

14. Gustafsson, S. E., 1991, "Transient Plane Source Technique for Thermal Conductivity and Thermal Diffusivity Measurements of Solid Materials", Review of Scientific Instruments, 62 (3), 797-804.

15. Gustavsson, M., H. Nagai and T. Okutani, 2003, "Thermal Effusivity Measurements of Insulating Liquids Using Microsized Hot Strip Probes", Review of Scientific Instruments, 74 (10), 4542-4548.

16. Gustavsson, M. and S. E. Gustafsson, 2006, "Thermal Conductivity as an Indicator of Fat Content in Milk", Thermochimica Acta, 442, 1-5.

17. Hammerschmidt, U., 2003, "A Quasi-Steady State Technique to Measure the Thermal Conductivity", International Journal of Thermophysics, 24 (5), 1291-1312.

18. Hammerschmidt, U. and V. Meier, 2006, "New Hot-Bridge Sensor to Measure Thermal Conductivity, Thermal Diffusivity, and Volumetric Specific Heat", International Journal of Thermophysics, 27 (3), 840-865.

19. Hooper, F. C. and F. R. Lepper, 1950, "Transient Heat Flow Apparatus for the Determination of Thermal Conductivities", Transactions of the ASHVE, 56, 309-324.

20. Kuntner, J., F Kohl and B. Jakoby, 2006, "Simultaneous Thermal Conductivity and Diffusivity Sensing in Liquids Using a Micromachined Device", Sensors and Actuators A, 130-131, 62-67.

21. MacInnes, J. M., X. Du and R. W. K. Allen, 2003, "Prediction of Electrokinetic and Pressure Flow in a Microchannel T-Junction", Physics of Fluids, 15 (7), 1992-2005.

22. Nix, G. H., G. W. Lowery, R. I. Vachon and G. E. Tanger, 1967, "Direct Determination of Thermal Diffusivity and Conductivity with a Refined Line-Source Technique", Progress in Astronautics and Aeronautics (G. G. Heller, ed.), Academic Press, New York, 865-877.

23. Van der Held, E. F. M. and F. G. Van Drunen, 1949, "A Method of Measuring the Thermal Conductivity of Liquids", Physica, 15 (10), 865-881.

24. Van der Held, E. F. M., J. Hardebol and J. Kalshoven, 1953, "On the Measurement of the Thermal Conductivity of Liquids by a Non-Stationary Method", Physica, 14, 208-216.

25. Voudouris, N. and K. Hayakawa, 1994, "Simultaneous Determination of Thermal Conductivity and Diffusivity of Foods using a Point Heat Source Probe: A Theoretical Analysis", Food Science and Technology, 27, 522-532.

26. Wang, C. Y. and M. L. Yang, 1995, "A New Calorimeter for Measuring Rapidly the Thermal Conductivity of Liquids", Thermochimica Acta, 255, 365-370.

27. Xie, H., H. Gu, M. Fujii and X. Zhang, 2006, "Short Hot Wire Technique for Measuring Thermal Conductivity and Thermal Diffusivity of Various Materials", Measurement Science and Technology, 17, 208-214.

28. Zhang, H., L. He, S. Cheng, Z. Zhai and D. Gao, 2003, "A Dual-Thermistor Probe for Absolute Measurement of Thermal Diffusivity and Thermal Conductivity by the Heat Pulse Method", Measurement Science and Technology, 14, 1396-1401.

29. Zhang, H., G. Zhao, H. Ye, X. Ge and S. Cheng, 2005, "An Improved Hot Probe for Measuring Thermal Conductivity of Liquids", Measurement Science and Technology, 16, 1430-1435.